Progress In Electromagnetics Research, Vol. 135, 105–122, 2013

A MULTI-SCALE LOCAL PHASE QUANTIZATION PLUS BIOMIMETIC PATTERN RECOGNITION METHOD FOR SAR AUTOMATIC TARGET RECOGNITION

Yikui Zhai[1, 2, *], Jingwen Li[1], Junying Gan[2], and Zilu Ying[2]

[1]School of Electronics Information and Engineering, Beihang University, Beijing, China

[2]School of Information and Engineering, Wuyi University, Jiangmen, Guangdong, China

Abstract—Synthetic aperture radar (SAR) automatic target recognition (ATR) has been receiving more and more attention in the past two decades. But the problem of how to overcome SAR target ambiguities and azimuth angle variations has still left unsolved. In this paper, a multi-scale local phase quantization plus biomimetic pattern recognition (BPR) method is presented to solve these two difficulties. By applying multiple scales local phase quantization (LPQ) on the observed SAR images, the blur and azimuth invariant features can be extracted, and these features are fusion at consecutive multiple scales to achieve better results. Then PCA method is applied to further reduce the feature dimension and achieve its efficiency. Finally, high dimensional space geometry covering method based on BPR theory is adopted to construct hyper sausage neuron links for target recognition. Experiments on the MSTAR database show that the proposed method can achieve satisfying recognition accuracy compared with other state-of-the-art methods.

1. INTRODUCTION

Nowadays, Synthetic Aperture Radar (SAR) is playing an important role in the field of military remote sensing because of its ability to imaging with high resolution under all-weather and all-time condition [1–5]. As a key application of SAR, automatic target recognition (ATR) based on SAR has a great value both in military and commercial applications. However, how to interpret the SAR images

Received 3 October 2012, Accepted 5 December 2012, Scheduled 12 December 2012

* Corresponding author: Yikui Zhai (yikuizhai@163.com).

and recognize the true targets correctly still remains to be studied and explored [6–16]. Currently, the proposed recognition methods for SAR targets are mainly template-based matching strategy [17] and model-based reconstruction method [18], together with the kernel-based method [19] which has been adopted for a wide range of applications because of its excellent performance. Recently, a multi-view joint sparse representation based SAR ATR method has been proposed and has achieved the state-of-the-art results [20]. However, many problems still haven't been perfectly resolved due to SAR image's special electromagnetic imaging process as a kind of coherent imaging radar. Generally, serious coherent wave speckle noise exists in the obtained SAR images, and distributions of targets and background have been considered for removing the noises [11]. But there are two main problems still left unsolved: one is the targets' azimuth angle orientation variation due to the uncertainty in imaging process; the other is the inevitable ambiguity (or blur) in SAR imaging due to its original imaging principle and design. For overcoming the problem of target azimuth angle variations, multiple classifiers for different azimuth angles are trained commonly and the azimuth of the probe target is needed to be estimated beforehand. However, these methods could not be applied in practice. For the second problem, to the best of our knowledge, SAR ATR methods presented did not consider the impact of ambiguity in recognition process and how to suppress it. Therefore, effective feature extraction and robust recognition method for overcoming the above two difficulties on SAR ATR has became a key issues.

In this paper, a multi-scale local phase quantization plus biomimetic pattern recognition (BPR) method to solve these two difficulties is presented. By applying local phase quantization (LPQ) on the SAR images, the blur and azimuth invariant features can be extracted. In nature and engineering practice, observation and analysis of objects are often carried by selecting different scales. Thus multiple scales are selected to extract and fuse the invariant features further for better results. However, multi-scale feature fusion brings the huge dimension feature problem. Here the simple principal component analysis (PCA) method is adopted to reduce the dimension and achieve the efficiency. Considering the azimuth angle variation of SAR targets, Biomimetic Pattern Recognition (BPR) [23] is introduced firstly to accomplish the SAR image recognition as a new application even though it has been widely used in fields of biometric recognition and has achieved outstanding performances [24]. According to BPR theory, the variation of azimuth angle of the same type targets can be considered as continuous variation, and the high dimensional space geometry

covering can be constructed by hyper neurons through best coverage of feature samples. So BPR method is suitable for modeling SAR targets azimuth angle variation recognition problem and can contribute to robust results for SAR ATR.

The rest of this paper is organized as follows. Section 2 introduces the ambiguities exist in synthetic aperture radar and the frequency domain based ambiguous and rotational invariant feature extraction method based on local phase quantization. Section 3 presents the proposed SAR recognition algorithm in the aspects of preprocessing procedure, multi-scale feature extraction process using multiple LPQ and BPR based recognition model. Section 4 presents and compares the experimental results on MSTAR database by choosing different parameters. Finally, Section 5 draws the conclusion of the paper.

2. AMBIGUOUS AND ROTATIONAL INVARIANT FEATURE EXTRACTION VIA LOCAL PHASE QUANTIZATION

2.1. Ambiguities in Synthetic Aperture Radar Images

The presence of range and azimuth (or Doppler) ambiguities in synthetic aperture radars (SARs) is due to its incoherent imaging principle and has been well proved [25–29]. These ambiguities can be classified as range ambiguities and azimuth ambiguities, which are shown as Figures 1 and 2. The first one is the response ambiguity at the receiver by the radar returns from two successive pulses overlaps when the pulse repetition frequency (PRF) is set too high, where the parameter of c and f_{PRF} in Figure 1 represent the velocity of light and PRF respectively. And the latter arises in SAR images from the finite sampling of the Doppler spectrum at the PRF. Since spectrum repeats at PRF intervals, the signal components outside this frequency interval fold back into the main part of the spectrum. In fact, the combination of range and azimuth ambiguities not only implies a lower limit on the required area of the physical antenna, but also challenges the post processing of SAR images.

From the theory of far-field antenna gain, the ambiguity-to-signal ratios (ASR) of SAR images can be evaluated theoretically. The radar return at a particular Doppler frequency f_0 and time delay τ_0

$$R(f_0,\tau_0) = \sum_{m,n=-\infty}^{\infty} G(f_0+m\mathrm{PRF},\tau_0+n/\mathrm{PRF})\cdot \sigma_A(f_0+m\mathrm{PRF},\tau_0+n/\mathrm{PRF}) \quad (1)$$

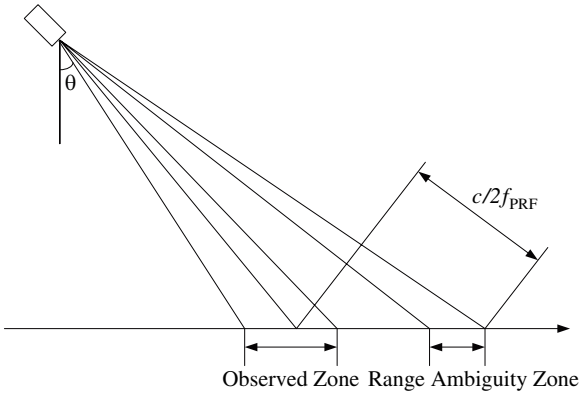

Figure 1. Illustration of range ambiguities generation.

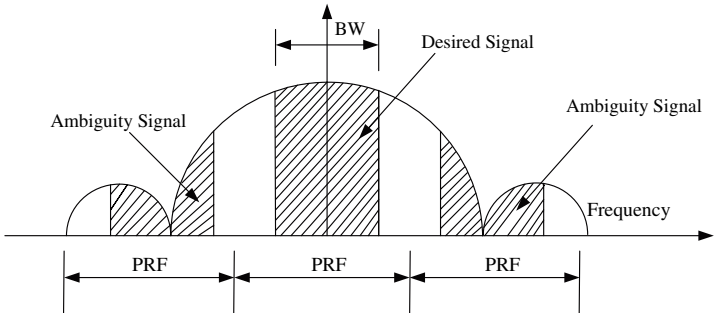

Figure 2. Illustration of azimuth ambiguities generation.

where m and n are nozero integers. PRF is the pulse repetition frequency, $G(f,\tau)$ the antenna gain pattern, and $\sigma_A(f,\tau)$ the radar reflectivity. The term with $m = n = 0$ is the signal and the rest of the terms constitute the ambiguity.

However, Equation (2) is difficult to evaluate in practice for two reasons. First, the antenna gain patterns are generally given as a function of the elevation and azimuth angle off the antenna boresight and not as a function of f and τ. Secondly, (2) is not suitable for computation because of the dependence of σ_A on range, angle of incidence, et al., are not explicitly indicated.

From the radar reflectivity and Ref. [28], many of the factors that appear in (2) can be cancelled out when one evaluates the ASR because they appear both in the signal and in the ambiguity calculation. In

fact, the ASR can be written as

$$\mathrm{ASR} = \frac{\sum_{m,n=-\infty}^{\infty} \int_{(-PBW)/2}^{(PBW)/2} G[e(f + m\mathrm{PRF}, \tau + n/\mathrm{PRF}), a\,(f + m\mathrm{PRF}, \tau + n/\mathrm{PRF})]\left[\sum(i)/R^4\right] df}{\int_{(-PBW)/2}^{(PBW)/2} G[e(f,\tau), a(f,\tau)]\left[\sum(i)/R^4\right] df} \tag{2}$$

The suppressing of ambiguities of SAR images has been studied for years. Ref. [25] suppress the azimuth ambiguity by designing ideal filters and canceling the ambiguity through multiple imaging, but the method is only suitable for the case of point scatters. Ref. [27] uses post-processing techniques to obtain ambiguity-free results. It requires the azimuth ambiguity zones to correspond to nulls in the azimuth antenna pattern. The energy in the nulls is considered to belong only to the main scene. A Wiener adaptive filter is then designed to reduce the ambiguity. Because the parameters of the filter, including the main scene and the ambiguity intensity, are estimated after imaging, the ambiguity removal effect relies on the properties of the scene, the precision of the imaging algorithms, and the antenna pattern measurement accuracy. Ref. [29] introduces compressed sensing for azimuth ambiguity suppression and presents two novel methods from the perspectives of system design and image formation, known as azimuth random sampling and ambiguity separation, respectively. However, for SAR automatic target recognition method, specific feature extraction method for suppressing the ambiguities has not been reported yet.

2.2. Frequency Domain Feature Extraction based on Local Phase Quantization

In this paper, contrary from designing of ideal filters for preprocessing the ambiguous SAR images, we considered extracting the ambiguous invariant local phase feature in frequency domain [30–33]. For SAR images, ambiguity of the observed image is inevitable due to the existence of range ambiguities and azimuth ambiguities. Thus the observed image $g(x)$ can approximately be expressed as a spatial convolution of the original image $f(x)$, given by

$$g(x) = f(x) * h(x) \tag{3}$$

where $h(x)$ is the point spread function (PSF) of the ambiguities, $*$ denotes 2-D convolution and x is a vector of image coordinates $[x,\, y]^T$. In the Fourier domain, this corresponds to

$$G(u) = F(u) * H(u) \tag{4}$$

where $G(u)$, $F(u)$, and $H(u)$ are the discrete Fourier transforms (DFT) of the blurred image $g(x)$, the original image $f(x)$, and PSF $h(x)$, respectively, and u is a vector of coordinates.

Since the radar is moved relatively to the target in SAR, we can assume the blur PSF $h(x)$ is centrally symmetric, namely $h(x) = h(-x)$, and as a consequence its phase can be given by

$$\angle H(u) = \begin{cases} 0, & \text{if } H(x) \geq 0 \\ -\pi, & \text{if } H(x) \leq 0 \end{cases} \tag{5}$$

Thus the phase of the observed image $\angle G(u)$ at the frequencies, where $H(u)$ is positive, is invariant to centrally symmetric ambiguity. It results that the original phase information of the observed SAR image by Fourier transform is remained unchanged.

To use the phase information, Short-Term Fourier Transform (STFT) is computed over a M by M local rectangular window N_x at each pixel x of the image $f(x)$ defined by

$$F(u, x) = \sum_{y \in N_x} f(x - y) e^{-j2\pi u^T y} \tag{6}$$

The responses at only four frequency points $u = [u_1, u_2, u_3, u_4]$ are considered in LPQ where $u_1 = [a, 0]^T, u_2 = [0, a]^T$, $u_3 = [a, a]^T, u_4 = [a, -a]^T$ and a is the frequency parameter. Let

$$F_x^c = [F(u_1, x), F(u_2, x), F(u_3, x), F(u_4, x)] \tag{7}$$

$$F_u = [\mathrm{Re}(F_x^c), \mathrm{Im}(F_x^c)]^T \tag{8}$$

where $\mathrm{Re}(\cdot)$ and $\mathrm{Im}(\cdot)$ return real and imaginary parts of a complex number, respectively. Thus, eight output response images are generated for a single image $f(x)$, four of which are real response images F_u^{Re} and the other four are imaginary response images F_u^{Im}. The quantized LPQ code for each pixel x is encoded into a decimal number between 0–255 as

$$\mathrm{LPQ}(x) = \sum_{i=0}^{3} \left(I(F_{u_i}^{\mathrm{Re}}(x)) \times 2^{2i} + I\left(F_{u_i}^{\mathrm{Im}}(x)\right) \times 2^{2i+1} \right) \tag{9}$$

where

$$I(x) = \begin{cases} 1, & x \geq 0 \\ 0, & \text{others} \end{cases} \tag{10}$$

Finally, a histogram h_f of these integer values from all pixels in image $f(x)$ is composed and used as a 256-dimensional feature vector.

3. THE PROPOSED METHOD

3.1. SAR Image Preprocessing Based on Centroid Location

To extract the region of interest (ROI) and eliminate the background noise, a simple image interception preprocessing procedure [19] is applied to the original SAR image. The method first locates the centroid of an SAR image

$$(x_c, y_c) = \left(\frac{m_{10}}{m_{00}}, \frac{m_{01}}{m_{00}}\right) \tag{11}$$

where

$$m_{pq} = \sum_x \sum_y x^p y^q f(x, y) \tag{12}$$

Here, (x, y) denotes a pixel's coordinate of the image and $f(x, y)$ denotes the pixel amplitude. After the centroid (x_c, y_c) is located, a $L \times L$ matrix is intercepted on the original SAR image centered at (x_c, y_c).

3.2. Improved Feature Extraction with Multi-scale Local Phase Quantization

In the proposed method, multi-scale LPQ is adopted to extract better features of SAR images. Multiple histograms of various scales by changing filter local window size M is calculated and concatenated into a single vector. Thus final multi-resolution descriptor for SAR image can be presented as follows

$$T_f = [h_{1,f}, h_{2,f}, \ldots, h_{\upsilon,f}] \tag{13}$$

where υ denotes the number of scales. Five LPQ images calculated at different scales where M is 13, 23, 33, 43, and 53 respectively is illustrated in Figure 3.

The multi-scale LPQ method can not only avoid the direct calculation on the amplitude information subjected to noise by quantifying the phase information in a local image window and interpret the SAR image at different scales, but also obtain more blur invariant and rotational invariant characteristics of the original SAR targets. For the high dimensionality and information redundancy brings by feature fusion, simple principal component analysis (PCA) method is adopted to extract the statistically independent information as a basis for BPR here.

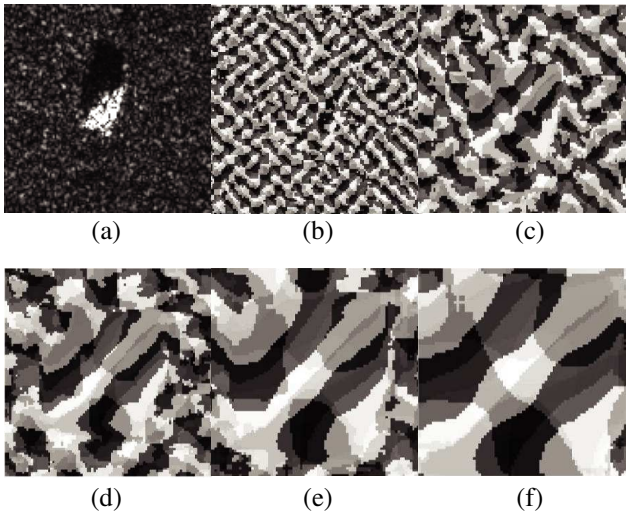

Figure 3. A SAR image (128×128) and its five scale LPQ resultant images (a)–(f).

3.3. The Proposed Algorithm Based on Biomimetic Pattern Recognition

Biomimetic Pattern Recognition (BPR) is introduced to the field of SAR target recognition as a new application. Compared with other pattern recognition methods, for instance Support Vector Machine (SVM) [21] which has been developed based on the concept of optimal separating hyper-plane, BPR emphasis on the process of learning which can be considered as the distinction between the learned samples and the infinite unlearned samples. Its theoretical basis is the continuity law of similar samples in the feature space. By applying the topology into the high dimensional feature space, it accomplishes the recognition process using the high dimensional geometry coverage. The basic principle of the theory can be described as the followed mathematical formula: In the feature space R_n, set A is assumed to include all the samples which belong to class A. And if there exits any two samples x and y in set A, then there must be a set B for any $\varepsilon > 0$:

$$\begin{aligned} B \;=\; & \{x_1, x_2, \cdots, x_n | x_1 = x, x_n = y, n \subset N, \rho(x_m, x_{m+1}) < 0, \\ & \varepsilon > 0 | n - 1 \geq\; m \geq 1,\, m \subset N)\} \end{aligned} \tag{14}$$

where $B \subset A, \rho(x_m, x_{m+1})$ is the distance between x_m and x_{m+1}.

Hence, azimuth angle variations of the same type target can be considered to be continuous in characteristic. For both the obtained

samples and those unknown samples from the same type, hyper neurons are selected to construct several hyper links in the purpose of best coverage. Thus it indicated that BPR is relative robust to the SAR target azimuth angle variation without estimating the azimuth angle in advance. In addition, the multi-scale approach also contributes to the final BPR recognition performance due to the high dimension feature information beneficial to geometry construction. BPR hyper sausage neuron links construction process is shown as Algorithm 1. The flowchart of the proposed SAR recognition algorithm is shown as Figure 4.

Algorithm 1. BPR Hyper Sausage Neuron Links Construction Process
Input: SAR target training set R (each class has N samples, and each sample is a $256 * 1$ feature vector)
Output: Hyper sausage neuron links of all training classes.
Start:
Step 1. For the first class in set R, find out the nearest two samples (i and j) among these N samples using Euclidean distance, that is $D_{ij} = \arg\min D_{xy}$, where D_{xy} means the distance from sample x to sample y. where $x, y \in \{1, 2, \ldots, N\}$.
Step 2. Build single hyper sausage neuron with sample i and sample j, and then calculate the Euclidean distances from the rest $N-2$ samples to the neuron. If there are any sample distances less than a threshold K, it is considered to be worthless samples and this sample should be discarded.
Step 3. After removing the worthless samples, calculate the distances again from the rest samples to the sample i and sample j, assuming that the newly added sample is k.
Step 4. Repeat Step 2 and Step 3 with j and k. A hyper sausage neuron link can be finally constructed after all N samples have been trained.
Step 5. Keep looping Step 1 to Step 4 until all classes in set R have been trained. In the end, hyper sausage neuron links of all training classes in R have been constructed.
End.

---

4. EXPERIMENTAL RESULTS

In the following experiments, the MSTAR SAR database provided by the US DARPA/AFRL MSTAR project team is used in order to

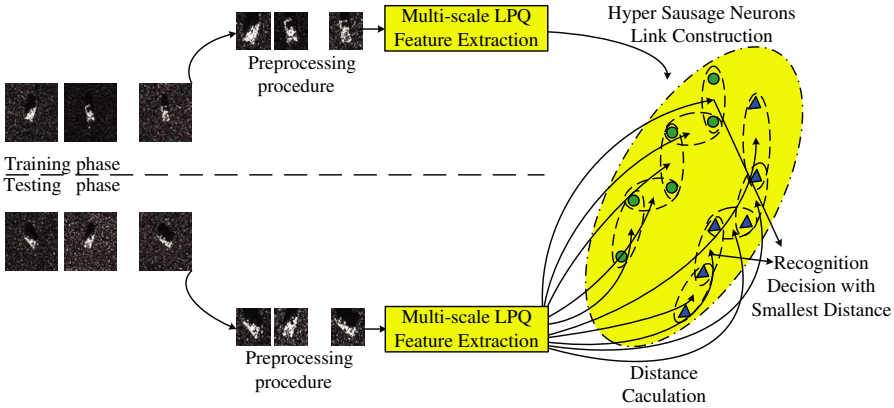

Figure 4. Flowchart of the proposed SAR recognition method.

Table 1. Configuration of three target types in MSTAR database.

Training Set	Number	Testing Set	Number
T72_SN132	232	T72_SN132	196
		T72_SN812	195
		T72_SNS7	191
BMP2_SNC21	233	BMP2_SN9563	195
		BMP2_SN9566	196
		BMP2_SNC21	196
BTR70_SNC71	233	BTR70_SNC71	196

evaluate the proposed algorithm's recognition performance. It was collected by Sandia National Laboratory in 1995 and 1996, respectively, using X-band, HH polarization, $0.3 \times 0.3\,\mathrm{m}^2$ high-resolution spotlight SAR [17]. The target set is divided into training set and testing set while both two sets contain multiple types of ground military target including T72 (Main Battle Tanks), BMP2 (Armored Personal Carriers), BTR70 (Armored Personal Carriers) etc.. The mentioned three targets' optical images and their SAR images are illustrated in Figure 5, and the configuration of them is shown as Table 1. The original size of each image chip is 128×128 and the variation of the azimuth angle of every type target in MSTAR database is from 0 to 360 degree, Figure 6 is the illustration of selected T72 SAR images rotated along the clockwise direction. Contrary from Ref. [17], the azimuth of targets are not classified beforehand for better results here.

(a) (b) (c)

Figure 5. Optical and observed SAR images of three targets in MSTAR: (a) T72, (b) BTR70, (c) BMP2.

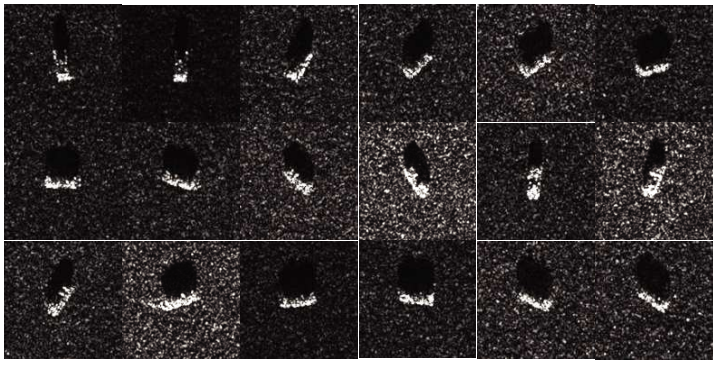

Figure 6. SAR target T72 with azimuth angle variations (0°–360°).

4.1. Experiments on Triple Scales for Selection of the Best Image Size L

From the observed SAR images shown in Figure 6, there are target and speckle noises in it. Thus preprocessing method is needed to perform to locate the region of interest (ROI) in order to reduce the impact of background noise and highlight the feature information of the ROI from the observed image. For MSTAR data, the ROI image size is assume to achieve best performance between the size value of 49 and 64. So these image sizes and the original image size are evaluated here in the experiments. Consecutive triple scales of LPQ are adopted to verify the best size for the proposed method. In view of the testing set

not including rejection targets and the purpose of checking the multi-scale approach's performance, the BPR method is only treated as a classifier rather than its inherent recognition function which can reject unlearned samples, without estimating the targets' azimuth angle in advance.

As Table 2 shows, 16 preprocessed image size values from 49 to 64 have been chosen to examine the recognition performance compared with image size 128×128. The best true recognition performance is achieved when the image size takes the value of 55. Table 3 gives the corresponding detailed scale value of local window size parameters for computing STFT in LPQ. It shows that the performance of $L = 128$ is not as good as the previous sizes which all have reached 90 percent recognition rate at least. Therefore, the above experimental results proved that the preprocessing procedure can improve the recognition rate by eliminating the background noise. In this paper, $L = 55$ is considered to be appropriate for multiple LPQ feature extracted and is adopted in the following experiment by its good performance.

Table 2. Performance of three target types under triple scale values fusion.

L/Index	True Recognition Rate (%)					
	1	2	3	**4**	5	6
49	90.88	92.06	93.6	94.52	95.38	95.55
50	92.12	93.09	93.49	94.8	95.43	95.15
51	92.64	92.75	93.6	94.92	96.17	95.21
52	92.41	93.78	94.23	95.60	95.66	95.66
53	92.41	93.72	94.46	95.66	96.12	95.15
54	92.35	94.29	94.46	95.94	96.00	95.43
55	92.70	93.83	94.92	**96.35**	95.89	95.09
56	93.10	93.95	95.26	96.06	95.20	95.20
57	93.38	94.23	95.89	95.83	95.26	94.86
58	93.50	94.35	95.66	95.77	95.37	95.09
59	93.72	94.52	96.06	95.72	95.43	94.75
60	93.78	95.15	96.23	95.03	95.49	94.35
61	93.55	95.09	96.06	95.09	95.37	94.06
62	93.84	95.15	95.89	95.49	95.49	94.18
63	94.18	95.26	96.23	95.26	94.57	94.01
64	94.36	95.15	96.06	95.37	94.46	94.29
128	87.59	87.13	87.94	86.01	86.46	84.99

Table 3. Detailed scale value corresponding to Table 2.

L/Index	Integrated Local Window Sizes $[M_1 M_2 M_3]$ Computed In LPQ					
	1	2	3	4	5	6
49–64	[33 31 29]	[31 29 27]	[29 27 25]	**[27 25 23]**	[25 23 21]	[23 21 19]
128	[53 51 49]	[51 49 47]	[49 47 45]	[47 45 43]	[45 43 41]	[43 41 39]

4.2. Experiments on Multi-scale LPQ and PCA for Efficient Feature Extraction and Dimension Reduction

By choosing consecutive integrated local window size Ms value, multiple integrated LPQ scales can be fusion as a feature descriptor. With the number of scales increasing, the dimension of a feature vector grows rapidly. High dimensionality can be benefited to the distribution of samples in the feature space and hence construct better geometry covering in order to improve the recognition rate. Experimental results of 8 scales LPQ fusion at most are shown in Table 4.

It is clear displayed that the performance of true recognition rate (TRR) has an overall upward trend with the increase of scale levels in Table 4. This trend shows that relative high feature dimensions can be conducive to the enhancement of the recognition rate. Table 4 also shows that the performance of T72, BMP2 and BTR70 by the proposed method can achieve a TRR of 94.33%, 96.59%, and 99.49% respectively. T72 and BMP2 achieve the worse result than BTR70 because of the existence of the other two variant configuration targets which are lack with training samples, while BTR70 has only one configuration with training samples which is easier for recognition. But it is proved that the proposed multi-scale method does work to improve the recognition rate of T72 and BMP2 increasing more than 4 percentages and 1 percentage, respectively.

However, high dimension feature vector brings the problem of long time consuming computation and information redundancy. Thus Principal Component Analysis (PCA) method is employed here to extract the statistically useful information and reduce the dimensionality of the original fusion feature. Experimental results of PCA based multi-scale LPQ is shown as Table 5. PCA dimension from 8 to 1280 is evaluated for 8 integrated scales LPQ here. As expected, the TTR rises with the output dimension increasing. And it reaches the highest true recognition rate 96.92% when the dimension set as 512. Comparing Table 5 with Table 4, we could find that the same best recognition result can be achieved at a lower cost by using PCA after the multi-scale approach, because the dimension of the highest TTR in Table 4 is 8×256 while only 512 in Table 5, which is four times

Table 4. Highest recognition result of various scale levels ($L = 55$).

Scale Level	True Recognition Rate (%)				Detailed Scale Value
	T72	BMP2	BTR70	MEAN	
1 scale	89.69	95.57	100.0	95.09	[23]
2 scales	91.41	95.23	100.0	95.55	[25 23]
3 scales	93.13	96.42	99.49	96.35	[27 25 23]
4 scales	92.27	95.57	100.0	95.95	[27 25 23 21]
5 scales	92.27	95.74	100.0	96.00	[27 25 23 21 19]
6 scales	92.78	95.4	99.49	95.89	[29 27 25 23 21 19]
7 scales	92.44	96.76	100.0	96.40	[27 25 23 21 19 17 15]
8 scales	**94.33**	**96.59**	**99.49**	**96.8**	**[27 25 23 21 19 17 15 13]**

Table 5. Recognition result of PCA dimension reduction on 8 scales LPQ.

Dimension	True Recognition Rate (%)			
	T72	BMP2	BTR70	MEAN
8	72.16	77.68	93.37	81.07
16	86.08	86.88	98.47	90.48
32	91.24	92.67	99.49	94.47
64	91.07	95.06	99.49	95.2
128	92.1	96.42	100.0	96.17
256	93.64	95.91	100.0	96.52
512	**94.33**	**96.42**	**100.0**	**96.92**
768	94.33	96.59	99.49	96.8
1024	94.33	96.59	99.49	96.8
1280	94.33	96.59	99.49	96.8

of the latter dimension. Thus it would save much precious time in the later decision process after applying the PCA method to the extracted multi-scale feature.

4.3. Comparison with Other Proposed Algorithms

To be more general, a comparison with other proposed algorithms is presented in Table 6. Among the listed algorithms, JSRC [20] is a novel kind of joint sparse representation based multi-view automatic target recognition method. Adaptive boosting algorithm is used in reference [22] to fuse the coarse and fine features extracted on targets

Table 6. Optimal recognition performance comparison of various proposed methods.

Recognition Methods	Accuracy
Template Matching [17]	40.76%
SVM [21]	90.92%
Single-View SRC [20]	92.30%
JSRC [20]	95.60%
Adaptive Boosting [22]	96.12%
Multi-scale LPQ+BPR	96.92%

to accomplish recognition. Compared with these five SAR recognition methods, the proposed multi-scale LPQ plus BPR method achieve better recognition performance in the case of no prior information of targets' azimuth angle. The significant improved performance shows that the combination of LPQ feature extraction method, multi-resolution representation and BPR recognition model outperforms other techniques.

5. CONCLUSION

A SAR automatic target recognition algorithm based on multi-scale Local Phase Quantization (LPQ) plus Biomimetic Pattern Recognition (BPR) has been proposed in this paper. Multi-scale representation is applied here to describe the phase information extracted by LPQ in a higher feature dimension and BPR is introduced to accomplish the high dimensional space geometry covering on training samples. Experimental results confirm that the proposed algorithm is a feasible and robust method for SAR image recognition. Moreover, PCA method is also adopted and verified by experiments in order to enhance the efficiency by reducing the feature dimension. However, the recognition performance of T72 and BMP2 still have large margin to be improved, so the variant configuration target recognition problem can be considered as a key issues in future research.

ACKNOWLEDGMENT

This work is supported by the National Natural Science Foundation of China under Grand No. 61072127, the Natural Science Foundation of Guangdong Province, P. R. China under Grand No. 10152902001000002, No. S2011040004211, No. S2011010001085

and No. 07010869, and Foundation for Distinguished Young Talents in Higher Education of Guangdong, China under Grand No. 2012LYM_0127.

REFERENCES

1. Huan, R. and Y. Pan, "Decision fusion strategies for SAR image target recognition," *IET Radar, Sonar and Navigation*, Vol. 5, No. 7, 747–755, 2011.
2. Lee, J.-H., S.-W. Cho, S.-H. Park, and K.-T. Kim, "Performance analysis of radar target recognition using natural frequency: Frequency domain approach," *Progress In Electromagnetics Research*, Vol. 132, 315–345, 2012.
3. Varshney, K. R., M. Cetin, J. W. Fisher, and A. S. Willsky, "Sparse representation in structured dictionaries with application to synthetic aperture radar," *IEEE Transactions on Signal Processing*, Vol. 56, No. 8, 3548–3560, 2008.
4. Chang, Y. L., C. Y. Chiang, and K. S. Chen, "SAR image simulation with application to target recognition," *Progress In Electromagnetics Research*, Vol. 119, 35–57, 2011.
5. Park, S. H., K. K. Park, J. H. Jung, H. T. Kim, and K. T. Kim, "Construction of training database based on high frequency RCS prediction methods for ATR," *Journal of Electromagnetic Waves Applications*, Vol. 22, Nos. 5–6, 693–703, 2008.
6. Chan, S. C. and K. C. Lee, "Radar target identification by kernel principal component analysis on RCS," *Journal of Electromagnetic Waves Applications*, Vol. 26, No. 1, 64–74, 2012.
7. Huang, C. W. and K. C. Lee, "Frequency-diversity RCS based target recognition with ICA projection," *Journal of Electromagnetic Waves Applications*, Vol. 24, Nos. 17–18, 2547–2559, 2010.
8. Jung, J. H. and H. T. Kim, "Comparisons of four feature extraction approaches based on fisher's linear discriminant criterion in radar target recognition," *Journal of Electromagnetic Waves Applications*, Vol. 21, No. 2, 251–265, 2007.
9. Sabry, R. and P. W. Vachon, "A spectral domain approach to modelling of EM scattering for synthetic aperture radar target recognition," *Journal of Electromagnetic Waves Applications*, Vol. 15, No. 6, 745–753, 2001.
10. Seo, D. K., K. T. Kim, I. S. Choi, and H. T. Kim, "Wide-angle radar target recognition with subclass concept," *Progress In Electromagnetics Research*, Vol. 44, 231–248, 2004.

11. Lee, K. C., C. W. Huang, and M. C. Fang, "Radar target recognition by projected features of frequency-diversity RCS," *Progress In Electromagnetics Research*, Vol. 81, 121–133, 2008.
12. Han, S. K., H. T. Kim, S. H. Park, and K. T. Kim, "Efficient radar target recognition using a combination of range profile and time-frequency analysis," *Progress In Electromagnetics Research*, Vol. 108, 131–140, 2010.
13. Lee, K. C., J. S. Ou, and M. C. Fang, "Application of svd noise-reduction technique to PCA based radar target recognition," *Progress In Electromagnetics Research*, Vol. 81, 447–459, 2008.
14. Huang, C. W. and K. C. Lee, "Application of ICA technique to PCA based radar target recognition," *Progress In Electromagnetics Research*, Vol. 105, 157–170, 2010.
15. Lee, K. C., J. S. Ou, and C. W. Huang, "Angular-diversity radar recognition of ships by transformation based approaches — Including noise effects," *Progress In Electromagnetics Research*, Vol. 72, 145–158, 2007.
16. Park, S. H., J. H. Lee, and K. T. Kim, "Performance analysis of the scenario-based construction method for real target ISAR recognition," *Progress In Electromagnetics Research*, Vol. 128, 137–151, 2012.
17. Ross, T. D., S. W. Worrell, V. J. Velten, J. C. Mossing, and M. L. Bryant, "Standard SAR ATR evaluation experiment using the MSTAR public release data set," *SPIE Conf. on Algorithms for SAR*, Vol. 3370, 556–573, 1998.
18. Zhou, J. X, Z. G. Shi, X. Chen, and Q. Fu, "Automatic target recognition of SAR images based on global scattering center model," *IEEE Transactions on Geoscience and Remote Sensing*, Vol. 49, No. 10, 3713–3729, 2011.
19. Han, P., R. B. Wu, Y. H. Wang, and Z. H. Wang, "An efficient SAR ATR approach," *Proc. of IEEE ICASSP*, Vol. II, 429–432, 2003.
20. Zhang, H. C., N. M. Nasrabadi, Y. N. Zhang, and T. S. Huang, "Multi-view automatic target recognition using joint sparse representation," *IEEE Transactions on Aerospace and Electronics Systems*, Vol. 48, No. 3, 2481–2497, 2012.
21. Zhao, Q. and J. C. Principe, "Support vector machines for SAR automatic target recognition," *IEEE Transactions on Aerospace and Electronics Systems*, Vol. 37, No. 2, 643–654, 2001.
22. Sun, Y. J., Z. P. Liu, S. Todorovic, and J. Li, "Adaptive boosting for SAR automatic target recognition," *IEEE Transactions on*

Aerospace and Electronics Systems, Vol. 43, No. 1, 112–124, 2007.

23. Wang, S. J., "Biomimetic pattern recognition — A new model of pattern recognition theory and its application," *Acta Electronica Sinica*, Vol. 30, No. 10, 2258–2262, 2002 (in Chinese).
24. Wang, S. J. and X. T. Zhao, "Biomimetic pattern recognition theory and its application," *Chinese Journal of Electronics*, Vol. 13, No. 3, 373–377, 2004.
25. Zhang, Z. and Z. S. Wang, "On suppressing azimuth ambiguities of synthetic aperture radar by three filters," *Proc. CIE — Int. Conf. Radar*, 624–626, 2001.
26. Villano, M. and G. Krieger, "Impact of azimuth ambiguities on Interferometric performance," *IEEE Geoscience and Remote Sensing Letters*, Vol. 9, No. 5, 896–900, 2012.
27. Guarnieri, A. M., "Adaptive removal of azimuth ambiguities in SAR images," *IEEE Transactions on Geoscience and Remote Sensing*, Vol. 43, No. 3, 625–633, 2005.
28. Li, F. K. and W. K. T. Johnson, "Ambiguities in spaceborn synthetic aperture radar systems," *IEEE Transactions on Aerospace and Electronic Systems*, Vol. 19, No. 3, 389–397, 1983.
29. Yu, Z. and M. Liu, "Suppressing azimuth ambiguity in spaceborne SAR images based on compressed sensing," *Science China — Information Science*, Vol. 55, No. 8, 1830–1837, 2012.
30. Ojansivu, V. and J. Heikkila, "Blur insensitive texture classification using local phase quantization," *International Conference on Image and Signal Processing, Lecture Notes in Computer Science, Springer*, Vol. 5099, 236–243, 2008.
31. Chan, C. H., J. Kittler, N. Poh, T. Ahonen, and M. Pietikainen, "(Multiscale) Local phase quantization histigram discriminant analysis with score normalisation for robust face recognition," *Workshop on Video-oriented Object and Event Classification, in Conjunction with IEEE Conference on Computer Vision*, 633–640, 2009.
32. Zhen, L. and S. Z. Li, "Fast multi-scale local phase quantization histogram for face recognition," *Pattern Recognition Letters*, Vol. 33, 1761–1767, 2012.
33. Rahtu, E., J. Heikkila, V. Ojansivu, and T. Ahonen, "Local phase quantization for blur-insensitive image analysis," *Image and Vision Computing*, 2012, doi:10.1016/j.imavis.2012.04.001.